Langmuir

Article

pubs.acs.org/Langmuir

Identification of Protein Domains on Major Pilin MrkA That Affects the Mechanical Properties of *Klebsiella pneumoniae* Type 3 Fimbriae

Chia-Han Chan,[†,○] Feng-Jung Chen,[‡,○] Ying-Jung Huang,[§] Shin-Yu Chen,[∥] Kuo-Liang Liu,[⊥] Zhe-Chong Wang,[§] Hwei-Ling Peng,[§] Tri-Rung Yew,[⊥] Cheng-Hsien Liu,[#] Gunn-Guang Liou,[▽] Ken Y. Hsu,[‡] Hwan-You Chang,*[,∥] and Long Hsu*[,†]

[†]Institute and Department of Electrophysics, [‡]Department of Photonics and Institute of Electro-Optical Engineering, and [§]Department of Biological Science and Technology, National Chiao Tung University, 1001 University Road, Hsinchu 300, Taiwan, Republic of China

[∥]Institute of Molecular Medicine and Department of Medical Science, [⊥]Department of Materials Science and Engineering, and [#]Department of Power Mechanical Engineering, National Tsing Hua University, 101 Section 2, Kuang-Fu Road, Hsinchu 300, Taiwan, Republic of China

[▽]Division of Molecular and Genomic Medicine, National Health Research Institutes, 35 Keyan Road, Jhunan, Miaoli County 350, Taiwan, Republic of China

Supporting Information

ABSTRACT: The *Klebsiella pneumoniae* type 3 fimbriae are mainly composed of MrkA pilins that assemble into a helixlike filament. This study determined the biomechanical properties of the fimbriae and analyzed 11 site-directed MrkA mutants to identify domains that are critical for the properties. *Escherichia coli* strains expressing type 3 fimbriae with an Ala substitution at either F34, V45, C87, G189, T196, or Y197 resulted in a significant reduction in biofilm formation. The *E. coli* strain expressing MrkAG189A remained capable of producing a normal number of fimbriae. Although F34A, V45A, T196A, and Y197A substitutions expressed on *E. coli* strains produced sparse quantities of fimbriae, no fimbriae were observed on the cells expressing MrkAC87A. Further investigations of the mechanical properties of the MrkAG189A fimbriae with optical tweezers revealed that, unlike the wild-type fimbriae, the uncoiling force for MrkAG189A fimbriae was not constant. The MrkAG189A fimbriae also exhibited a lower enthalpy in the differential scanning calorimetry analysis. Together, these findings indicate that the mutant fimbriae are less stable than the wild-type. This study has demonstrated that the C-terminal β strands of MrkA are required for the assembly and structural stability of fimbriae.

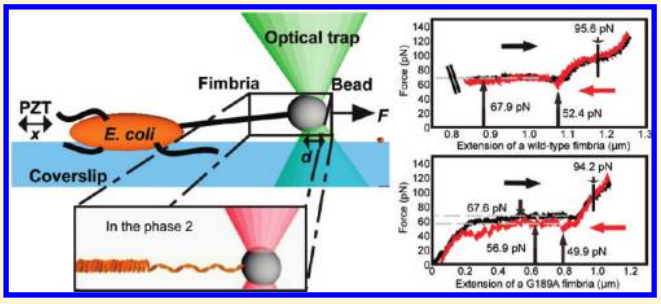

1. INTRODUCTION

Bacterial fimbriae are hairlike appendages that play critical roles in bacterial motility, gene transfer, and pathogenesis. Via fimbriae, bacteria can attach to the host epithelium, and the specific adhesion allows them to resist the drag forces arising from aqueous flushes in the urinary and gastrointestinal tracts.[1−3] The significance of flexibility and elasticity of fimbriae in the bacterial attachment to host cells has been demonstrated in P-type fimbriae,[4,5] type 1 fimbriae,[6−8] and type 3 fimbriae.[9]

Fimbriae are generally several nanometers in diameter and 1 to 2 μm in length and display a helical springlike structure.[10,11] A fimbria typically consists of a few thousand pilins linked to an adhesin molecule at the distal end for host cell attachment. Many fimbriae, including the type 3 fimbriae, are assembled via the chaperon/usher pathway. The chaperon−pilin and the pilin−pilin interactions are crucial for fimbriae assembly and are attributed to certain sequence features of pilins, such as a disulfide bond between two conserved Cys residues[12] and a hydrophobic groove in the C-terminal region of pilins.[13,14] The N-terminal region from residues 12−20 of the P-type fimbriae major pilin PapA is required for the fimbriae to coil into a helix.[15] Similarly, the disruption of the loop region of PapA (residues from 106 to 109) also abolishes the helical rod structure, leading to a linear fiber.[16] In addition, a change in the adhesin-binding activity by the coexpression of different major pilin variants has been demonstrated.[17]

The force required to uncoil the fimbrial shaft is a major physical feature of a fimbria that can be determined using technology such as optical tweezers. The uncoiling force is highly dependent on the interaction of major pilins as demonstrated previously in three different types of fimbriae.[9] An apparent change in the uncoiling force under salinity or pH

Received: January 16, 2012
Revised: April 17, 2012
Published: April 23, 2012

treatments was demonstrated in the P-type fimbriae.[18] The characteristic force is another physical feature of fimbriae that is defined as the force at the inflection point of the S-shaped force−extension curve of a fimbria. The characteristic force is independent of the fimbrial length and the extension speed.[9] In addition to the stretching properties of fimbriae, the P-type fimbriae displayed rapid contractibility, a property likely essential for the adherence of the uropathogenic *Escherichia coli* to urethra epithelium under urine flow.[19]

Differential scanning calorimetry (DSC) has also been used to characterize the structural and thermodynamic features of fimbriae quantitatively. A DSC measurement of the intermolecular interaction of the F4 fimbriae showed that the conformational change of the major pilins by means of a donor−strand complementation/exchange mechanism is crucial to fimbrial assembly.[20] Another DSC measurement of the intramolecular interaction of pilins demonstrated that a disulfide bond is essential for the stability of the Dr fimbriae.[21]

Klebsiella pneumoniae is a common nosocomial pathogen causing both pneumonia and urinary tract infections.[22] Most *K. pneumoniae* clinical isolates essentially carry the type 3 fimbriae encoding genes *mrkABCD*.[23] The adhesion filaments have been reported to be able to adhere to the epithelial cells from the respiratory and urinary tracts as well as to extracellular matrix proteins collagen IV and V.[1,24,25] Although the receptor has not yet been identified, we have previously used optical tweezers to measure the adhesive forces of the adhesion molecules MrkD to collagen with a resolution reaching pico-Newtons.[26]

Several reports have also demonstrated that type 3 fimbriae are crucial for *K. pneumoniae* to form a biofilm,[27−29] a complex aggregation of microorganisms essential for bacterial colonization. The major pilin MrkA but not the adhesion molecule MrkD has been shown to play a major role in biofilm formation.[30] The overall sequence identity between MrkA and other pilins, such as FimA, PapA, LpfA, and MrpA, was relatively low, indicating that the type 3 fimbriae may have mechanical properties that are distinct from those of other fimbriae. In the current study, we went further to elucidate the structure−function relationship of MrkA, the major pilin of the type 3 fimbriae. Site-directed mutagenesis was performed on MrkA at 11 conserved residues. The recombinant bacterial strains expressing mutant MrkA were analyzed for their activities in type 3 fimbriae production and biofilm formation. Finally, the effects of these amino acid substitutions on the fimbriae backbone stability were also determined using optical tweezers and DSC.

2. EXPERIMENTAL SECTION

2.1. Site-Directed Mutagenesis. The recombinant plasmid p*mrkABCD* for type 3 fimbriae expression was previously constructed, and the nucleotide sequence was determined.[31] The mutations of *mrkA* were introduced using the QuikChange site-directed mutagenesis method (Stratagene, Agilent Technologies, Santa Clara, CA) according to the manufacturer's protocols. The primers used in this study are listed in Table S1 in the Supporting Information. After verification with nucleotide sequencing, the resulting plasmids were individually transferred into *E. coli* JM109, and the recombinant bacteria were grown at 37 °C in Luria−Bertani (LB) broth supplemented with 100 μg/mL ampicillin.

2.2. Biofilm Formation. Biofilm formation was analyzed as described elsewhere with minor modifications.[32] Bacteria grown overnight were diluted at a 1:100 ratio in LB broth, inoculated into each well of a 96-well microtiter plate, and incubated at 37 °C for 48 h. After the bacterial culture was removed, 120 μL of 1% (w/v) crystal violet was added to each well and incubated at room temperature for 15 min. The 96-well plate was then washed with water, the dye on each well was solubilized in 95% ethanol, and the absorbance at 595 nm was determined using an enzyme-linked immunosorbent assay reader (ELx800, BioTek Instruments, Winooski, VT).

2.3. Detection of Bacterial Fimbriae Production with Gel Electrophoresis. To evaluate the assembly of MrkA into type 3 fimbriae, 150 μL of overnight-grown recombinant bacteria was centrifuged for 1 min at 4000*g*. The pellets were mixed with 50 μL of loading buffer (100 mM Tris-HCl pH 8.0, 4% SDS, 0.2% bromophenol blue, 2% β-mercaptoethanol, 20% glycerol), left undisturbed at room temperature for 30 min, and then resolved with 2.5% sodium dodecyl sulfate/7.5% (w/v) polyacrylamide gel electrophoresis (SDS-PAGE), followed by Western blotting analysis using an anti-MrkA polyclonal antibody. The duplicate samples were boiled for 10 min, resolved on 2.5% SDS-12.5% PAGE, and probed with the anti-MrkA antibody for the determination of the total quantity of MrkA monomer.

2.4. Transmission Electron Microscopy Examination. The preparation of bacterial specimens for transmission electron microscopy (TEM) examination was described previously.[33] Briefly, 2.5 μL of *E. coli* in LB broth was adsorbed onto a glow-discharged grid, washed with distilled water, stained with 2% (w/v) uranyl acetate, and air dried for later inspection. An H7650 transmission electron microscope (Hitachi, Tokyo, Japan) operated at an acceleration voltage of 80 kV and a Tecnai G^2 Spirit TWIN (FEI Company, Hillsboro, OR) operated at an acceleration voltage of 120 kV were used in this study. The TEM images from the H7650 at magnifications of 15 000× and 150 000× were recorded using a digital camera system. The TEM images from the Spirit TWIN were recorded at magnifications of 2100× and 42 000× using another digital camera system.

2.5. Optical Tweezers Setup and Sample Preparation for the Mechanical Property Measurement. The recombinant *E. coli* grown in LB broth was centrifuged for 1 min at 9000*g*, washed twice with phosphate-buffered saline (PBS; 137 mM NaCl, 2.7 mM KCl, 10 mM Na_2HPO_4, and 2 mM KH_2PO_4), and then resuspended in PBS. The protein A-carboxyl latex beads (1 μm in diameter, Polysciences, Warrington, PA) previously washed with the protein A/G buffer (0.1 M Tris-HCl and 0.15 M NaCl) were incubated with a polyclonal antibody specific to the adhesin MrkD at 4 °C for 1 h, washed with the protein A/G buffer again, and then resuspended in PBS. No interaction was observed between bacteria expressing type 3 fimbriae and beads without an antibody coating. The coverslips were thoroughly rinsed with deionized water and dried completely before use.

The device for the fimbriae measurement with optical tweezers consisted of two coverslips spaced ∼170 μm apart with double-sided tape. A fresh *E. coli* suspension in PBS was injected into the space between the coverslips and left undisturbed for 1 min, and then the PBS was drained and the bacteria were left for an additional 30 min to ensure their immobilization on the coverslip. Subsequently, anti-MrkD antibody-modified beads in PBS were meticulously injected into the space. The prepared sample was immediately placed into the optical tweezers sample holder and left for 1 h prior to measurements.

The optical tweezers system used in this study has been described in detail.[9,26] Conceptually, a trapping laser was used to trap a bead. A probing laser was used to detect force-dependent displacements of the trapped bead. The system was calibrated using a power spectral density method with a correlation of Faxén's law.[34]

After the immobilization of most bacteria on the bottom of a sample was confirmed, a surface-modified bead was trapped for calibration using the power spectral density method. The stiffness of the trapping force on the bead was typically 750 pN/μm. Then the calibrated bead was moved near a bacterium, and the adhesion of some type 3 fimbriae to the bead was awaited. Finally, the trapped bead was moved away from the bacterium at a speed of 0.01 μm/s by a piezoelectric stage and the force required for the movement was recorded. At the end of pulling, the bead was allowed to return to its original position at the

dx.doi.org/10.1021/la300224w | *Langmuir* 2012, 28, 7428−7435

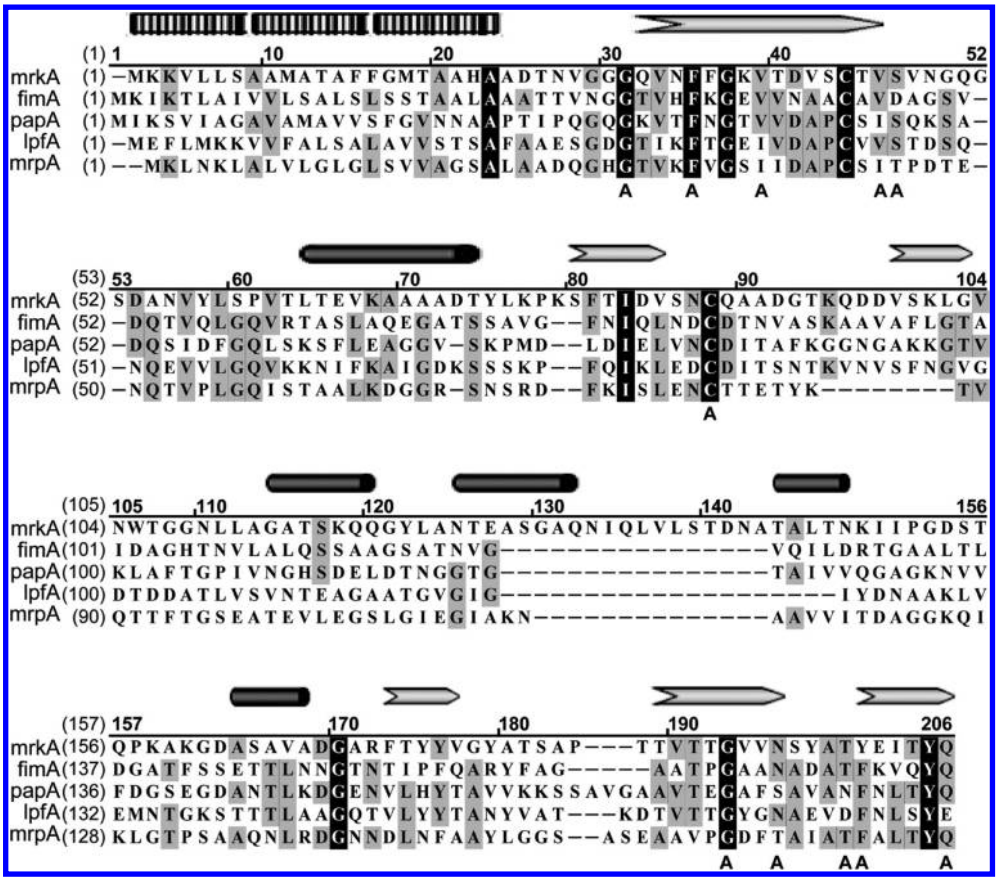

Figure 1. Protein sequence comparison between MrkA and other major pilins. The pilin sequences for comparison are MrkA, *K. pneumoniae* type 3 fimbriae; FimA, *E. coli* type 1 fimbriae; PapA, *E. coli* P fimbriae; LpfA, *Salmonella typhimurium* Lpf fimbriae; and MrpA, *Proteus mirabilis* PMF fimbriae. Residues with black boxes indicate identical residues, and those shaded gray indicate similar residues. The putative signal peptide (sequence of small rectangles), α helix (gray arrows), and β strand (solid black cylinders) are labeled on top of the sequences, and the substituted residues are marked "A" below.

same speed by the piezoelectric stage and the force was recorded similarly.

2.6. Differential Scanning Calorimetry (DSC) Measurements of Recombinant Fimbriae. The purification of type 3 fimbriae for DSC analysis was performed as described previously with minor modifications.[35] Briefly, recombinant bacteria expressing different MrkA variants were propagated in 100 mL of LB broth for 20 h and collected by centrifugation for 10 min at 11 000*g* and then resuspended in 30 mL of PBS. The suspension was held at 60 °C for 1 h and centrifuged for 10 min (11 000*g*, 4 °C), and then ammonium sulfate was added to the supernatant to a final concentration of 40% (w/v). The fimbriae were collected by centrifugation for 10 min at 11 000*g*, and the pellets containing type 3 fimbriae were dried overnight in a vacuum for later use. The purity of the fimbriae preparation was determined by SDS polyacrylamide gel electrophoresis and Commassie blue staining as shown in Figure S1 (Supporting Information). Thermal gravimetric analysis was performed on a TGA-7 Perkin-Elmer calorimeter (Perkin-Elmer, Waltham, MA) under argon flow (20 mL/min) at a temperature-increasing rate of 10 °C/min. In addition, thermal analysis was carried out by using a DSC instrument (Q-20, TA Instruments, New Castle, DE) under an atmosphere of dry N_2. All samples (weight 2 to 3 mg, sealed in an aluminum pan) in the DSC experiments were heated from −90 to 150 °C at a scanning rate of 20 °C/min and then quenched to −90 °C to repeat the same scanning procedure.[36]

3. RESULTS

3.1. Site-Directed Mutagenesis of *mrkA*. Because precise structural information of the major pilin MrkA is lacking, multiple sequence alignment was performed to identify evolutionally conserved sequences in the protein that may be critical to its function (Figure 1). Site-directed mutagenesis was subsequently performed on MrkA at 11 amino acid residues on the basis of three criteria:[12] (1) highly conserved residues (G30, F34, V38, C87, G189, and Y197) that have been proposed to facilitate major pilin interaction, (2) two conserved residues (V45 and S46) located within a critical Cys−Cys loop between residues 43 and 87, and (3) three conserved residues (N192, T196, and Q202) that may mediate hydrophobic groove formation in major pilins.[13] These selected residues were successfully substituted with an Ala; the mutated site was verified by nucleotide sequencing and denoted as G30A, F34A, V38A, V45A, S46A, C87A, G189A, N192A, T196A, Y197A, and Q202A, respectively.

3.2. Biofilm Formation of the Recombinant Bacteria Expressing MrkA Variants. The biofilm-forming activity was evaluated using the bacterial strains expressing a mutant MrkA to examine the effects of the site-directed mutations. As shown in Figure 2, recombinant *E. coli* JM109[p*mrkABCD*] strains harboring a MrkA variant, including G30A, V38A, S46A, N192A, and Q202A, exhibited strong biofilm-forming activity comparable to that of the wild-type strain. In contrast, strains carrying either an F34A, V45A, C87A, G189A, T196A, or Y197A mutation displayed significantly less biofilm-forming activity.

3.3. Effects of the *mrkA* Mutations on Pilin Polymerization. To elucidate whether the poor biofilm formation of

dx.doi.org/10.1021/la300224w | *Langmuir* 2012, 28, 7428−7435

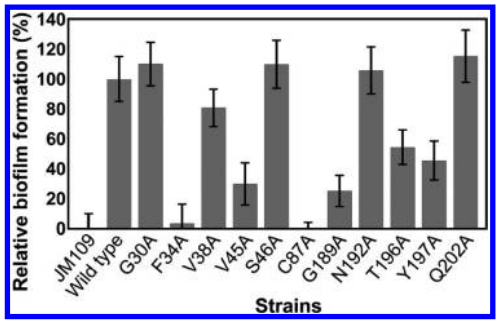

Figure 2. Biofilm formation by the *E. coli* strains expressing different MrkA variants. The recombinant *E. coli* strains were incubated on a 96-well polystyrene microtiter plate for 48 h. The biofilm formed by the bacteria was stained with crystal violet, dissolved in ethanol, and quantified photometrically at 595 nm. Results represent the mean and standard deviation of three independent experiments. Each value (in percentage) was derived from the ratio of the absorbance of each strain to that of the wild-type strain.

these mutants was due to the inability to assemble fimbriae, Western analysis using a MrkA-specific antibody was performed. Figure 3 shows that all of the tested recombinant

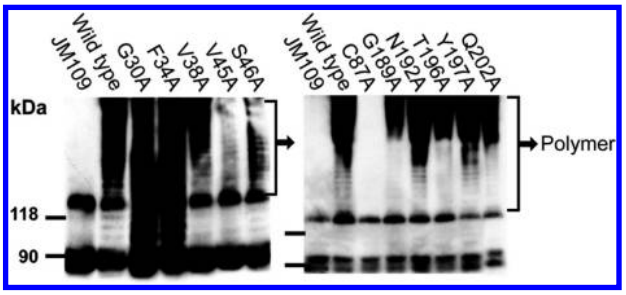

Figure 3. Formation of polymeric MrkA in *E. coli* strains expressing different MrkA variants. The cell lysates from the recombinant *E. coli* were resolved with 2.5% SDS/7.5% (w/v) PAGE and subjected to Western blotting analysis using an anti-MrkA polyclonal antibody. The polymeric form of the MrkA protein is not observed on either *E. coli* JM109 or *E. coli* expressing the MrkAC87A mutant.

bacterial strains, except that expressing MrkAC87A, produced fimbriae with polymeric patterns similar to that of the wild-type strain. This finding indicates that the mutation at the C87 residue prohibited MrkA from assembling into a polymeric form.

The gross morphology and quantity of the fimbriae produced by the *mrkA* mutant bacterial strains were examined further using TEM. The recombinant *E. coli* JM109[p*mrkABCD*] strains produced approximately 700 fimbriae (n = 3) with an average length of 1.5 ± 0.6 μm (n = 290, Figures 4 and 5a). Consistent with the results from the polymer pattern analysis, no fimbria was detected on the C87A mutant cells (Figure 5b), again indicating that residue C87 is essential to assembling MrkA subunits into a filament form. Although the average length and diameter of most of the mutant fimbriae appeared to be similar to those of the wild-type strain (Figures 4b,c and S2–S12 in the Supporting Information), a reduction in the fimbrial number was found in V45A, T196A, and Y197A mutants (~200 fimbriae/cell, Figure 5c) and F34A mutants (~100 fimbriae/cell, Figure 4a). Interestingly, many fimbrial fragments were frequently found near the V45A and T196A cells (Figure 5d,e), suggesting that these mutations affect the structural stability of the type 3 fimbriae.

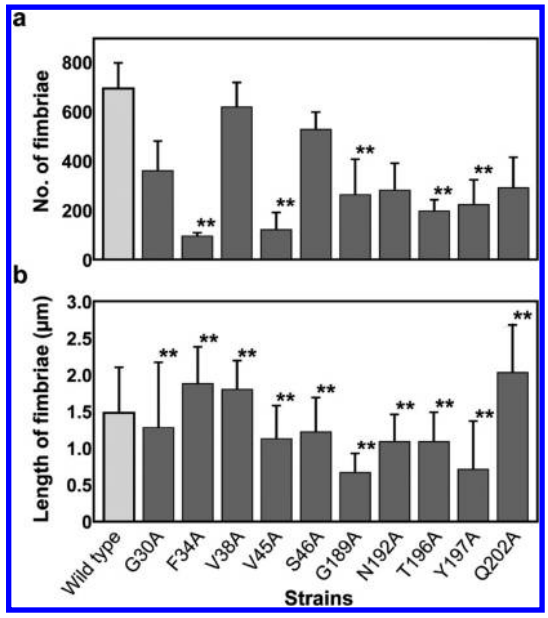

Figure 4. Effects of the site-specific substitution at MrkA on the (a) quantity and (b) length of the fimbriae. The average number and length of the fimbriae produced by the recombinant *E. coli* strain carrying a mutation together with the standard deviations ($n \geq 3$ bacteria for panel a and $n \geq 100$ fimbriae for panel b) are shown. The statistical significance of each mutant versus the wild type was determined by the Student t test (**$P < 0.01$). The MrkAC87A mutant does not produce any fimbriae; therefore, the data are not shown.

3.4. Stretching Property of the Recombinant G189A Type 3 Fimbriae. The optical tweezers method was used to determine the force–extension curve (FEC) of the MrkA mutant fimbria to elucidate the effects of the mutations on the elasticity and stability of the fimbria. The optical tweezers measurements revealed that all of the recombinant fimbriae, except the G189A fimbriae, exhibited a typical three-phase extension (Figure 6a), as demonstrated previously for the wild-type type 3 fimbriae.[9] The three typical phases are (1) a nonlinear extension with increasing forces in the first phase, (2) a constant uncoiling stage with a force ranging from approximately 60 to 70 pN (Table S2 in the Supporting Information), and (3) an S-shaped FEC exhibiting a characteristic force of 98 pN at the inflection point in the third phase. The G189A fimbriae exhibited an FEC that was distinct from that of the wild-type fimbriae (Figure 6b). In phase 1, a stretching force imposed on the G189A fimbria was proportional to the fimbrial extension with a spring constant of 224.6 pN/μm. Getting into phase 2, the stretching force continuously increased following another spring constant of 30.3 pN/μm, and then maintained a fixed force level of 67.6 pN, similar to the uncoiling force of the wild-type fimbria (~66 pN, Table S2 in the Supporting Information).

3.5. Contractibility of the Wild-Type and the MrkAG189A Fimbriae. The effects of the G189A substitution on the contractibility of the type 3 fimbriae were also determined. As shown in Figure 7a, the wild-type fimbriae contracted readily after being stretched, following the three-phase stretching pattern in a reverse fashion. Specifically, when the wild-type fimbria contracted from the third phase back to the second phase, the contracting force followed the stretching tendency in reverse until the bacterium-to-bead separation was

dx.doi.org/10.1021/la300224w | *Langmuir* 2012, 28, 7428–7435

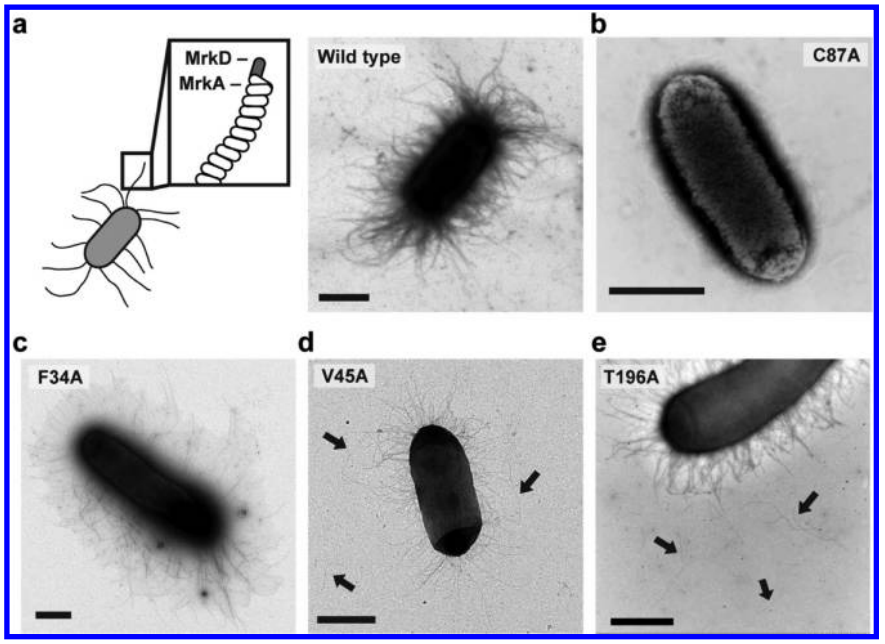

Figure 5. TEM images of the type 3 fimbriae-expressing *E. coli* strains. (a) *E. coli* JM109 expressing type 3 fimbriae with wild-type MrkA. The left part is a schematic illustration of the bacterium expressing the fimbriae composed of a tip-located adhesin MrkD and major pilins MrkA from the right part. (b) *E. coli* JM109 expressing the MrkAC87A mutant. No fimbria was observed on the cell. (c) *E. coli* JM109 expressing type 3 fimbriae with the MrkAF34A mutant. Relatively few abundant fimbriae (~100) were detected. Recombinant *E. coli* expressing (d) MrkAV45A and (e) MrkAT196A are shown. Some detached or fragmented fimbriae as indicated with arrows were found surrounding the bacterial cells. All scale bars are 1 μm.

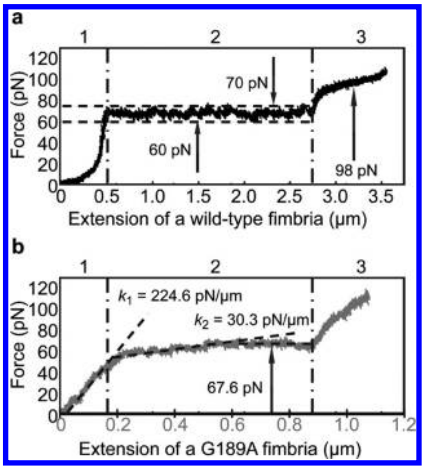

Figure 6. Stretching behaviors of the type 3 fimbriae expressed on *E. coli*. The FECs were measured with optical tweezers. (a) Typical three-phase FEC of a wild-type fimbria. All of the recombinant fimbriae, except the G189A fimbriae, exhibited similar behavior. The measured uncoiling forces of individual recombinant fimbriae ranged from 60 to 70 pN. (b) FEC of the G189A fimbriae. In phase 1, the stretching force was proportional to the fimbrial extension with a spring constant of 224.6 pN/μm. Getting into phase 2, the stretching force proportionally increased with another spring constant of 30.3 pN/μm and then suddenly fixed at a force level of 67.6 pN.

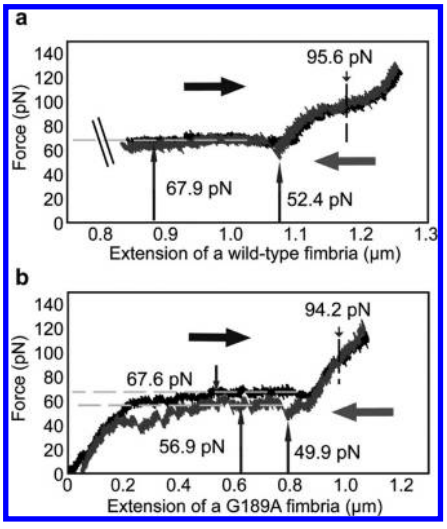

Figure 7. Stretching and contracting behaviors of the type 3 fimbriae expressed on *E. coli* cells. The stretching FEC (→) and contracting FEC (←) of a wild-type fimbria or that of a G189A fimbria are shown by a black curve and a gray curve, respectively. (a) Wild-type fimbria displayed an uncoiling force as well as a recoiling force of 67.9 pN, a characteristic force of 95.6 pN, and a nucleated force of 52.4 pN as indicated by arrows. (b) G189A fimbria displayed an uncoiling force of 67.6 pN, a recoiling force level of 56.9 pN, a characteristic force of 94.2 pN, and a nucleated force of 49.9 pN as indicated by arrows.

1.08 μm as indicated in Figure 7a. Hysteresis, which occurred during the separation from 1.08 μm down to 1.06 μm as shown in Figure 7a, may result from incorrect recoiling between MrkA pilins. However, when the contracting force decreased to 52.4 pN, certain layer-to-layer MrkA molecular interactions started to form and served as nucleation kernels to trigger additional layer-to-layer bonds successively. The contracting force at this trigger moment is called a nucleated force. After the separation was shortened to 1.06 μm (Figure 7a), the contracting force of the fimbria jumped to 67.9 pN, comparable to the typical uncoiling force (66 pN, Table S2 in the Supporting Information), and then the fimbria started recoiling until its nonstretched structure was recovered.

The G189A fimbria also adopted a three-phase contraction behavior, although it is distinct from its stretching FEC,

dx.doi.org/10.1021/la300224w | *Langmuir* 2012, 28, 7428–7435

particularly in the second phase (Figure 7b). When the G189A fimbria contracted from the third phase back to the second phase, the contracting force followed the reversed stretching tendency to a separation of 0.9 μm, as shown in Figure 7b. However, unlike the wild-type fimbria, the contracting FEC of the MrkAG189A fimbria had more than one hysteresis occurring during the bacterium-to-bead separation from 0.9 to 0.2 μm (Figure 7b). The first nucleated force was 49.9 pN at a separation of 0.8 μm. After the separation, the fimbria continued to contract to recoil on a force level of 56.9 pN but accompanied by several hystereses, revealing the unstable contractibility of the MrkAG189A fimbria.

3.6. Thermal Unfolding of Recombinant Fimbriae. The thermal unfolding of wild-type fimbriae and MrkAG189A mutant fimbriae was performed using DSC to examine the differences in their structural stability. As shown in Figure 8, the

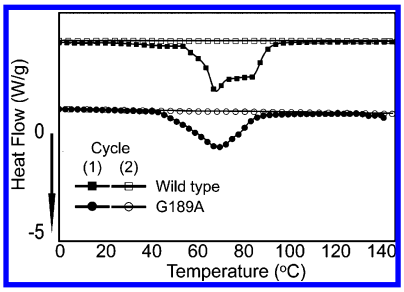

Figure 8. Thermodynamic profiles of the wild-type fimbriae and G189A fimbriae measured using DSC analysis. The two thermograms, ranging vertically for clarity, individually show a clear endothermic peak when temperature was increased from 0 to 140 °C in the first heating process. At these peaks, the particular temperatures assigned to the wild-type fimbriae and G189A fimbriae are 68 and 70 °C, respectively. The thermograms of all of the samples during the second heating process became flat and featureless. All of the DSC experiments were carried out three times using three independently prepared fimbrial samples.

thermal profiles of the two types of fimbriae exhibited a clear endothermic peak in the first heating process. The temperature at the peak is conventionally called the melting temperature (T_m). The T_m for the MrkAG189A mutant is reproducibly determined to be 70 °C, which is slightly higher than that of wild-type MrkA (68 °C, Table 1). After the same heating

Table 1. Melting Temperature (T_m) and Enthalpy (ΔH) of the Wild Type and G189A Mutant of Type 3 Fimbriae

	T_m (°C)	ΔH (J/g)
wild type	68	73.4
MrkAG189A	70	37.8

process was repeated, the DSC thermograms for both fimbriae became flat and featureless, suggesting that thermal denaturation occurred during the first heating process. The enthalpy of the thermal denaturation transition of a sample can be derived from the product of the area enclosed by the two successive curves in DSC thermograms and a calorimetric constant. The calorimetric constant depends on the instrument used and can be determined by analyzing a well-characterized sample with a known enthalpy. On the basis of this principle, the derived enthalpy of the MrkAG189A mutant fimbriae was smaller than that of the wild-type fimbriae (37.8 vs 73.4 J/g, Table 1).

4. DISCUSSION

The inability of the *E. coli mrkAC87A* strain to produce the type 3 fimbriae, as determined by gel electrophoresis and direct TEM examination, suggests that C87 is critical for MrkA to be assembled into a polymeric form. In the case of PapD, the Cys residue corresponding to C87 in MrkA has been proposed to form a disulfide bond with C43 through disulfide isomerase DsbA. The formation of the disulfide bond is also essential for the pilin to interact with chaperons to stabilize and transport the PapD subunits across the periplasm.[37] The reason that the MrkAC87A monomer was also absent for the whole cell lysate of the mutant cells is unclear (Figure S13 in the Supporting Information). Because the nucleotide sequence of the expression plasmid has been verified, we speculated that the MrkAC87A molecule becomes misfolded in the absence of the C43−C87 disulfide bond and is subjected to proteolytic degradation.

Several *mrkA* mutations including F34A, V45A, T196A, and Y197A did not affect the fimbriae assembly remarkably, although the biofilm-forming activity of the *E. coli* strains expressing these MrkA variants was clearly reduced. Fimbriae assembly through the chaperon/usher pathway is typically achieved by donor−strand complementation during the chaperon−pilin interaction and by donor−strand exchange during the pilin subunit−subunit interaction. In both Fim and Pap fimbriae, the two interaction mechanisms involve residues in both the N-terminal and C-terminal β strands of the major pilins.[13,14] Most major pilins possess an N-terminal extension, which contains a motif of alternating hydrophobic residues (P2−P5 residues) able to insert the corresponding P2−P5 binding pockets in the hydrophobic groove of an adjacent subunit during the donor−strand exchange process.[38] Residues F34 and V38 of MrkA are located at the sites corresponding to the PapA P3 and P5 residues, respectively.[39] The F34A substitution may influence the donor−strand exchange reaction and accordingly reduce the stability and quantity of the fimbriae displayed on cells. However, the V38A substitution did not significantly affect the assembly of type 3 fimbriae despite the P5 residue of major pilins being regarded as essential to initiating the donor−strand exchange reaction.[38] However, residue V45, which is an equivalent of residue I24 located on the A1 β strand of PapA, may involve the donor−strand complementation reaction.[13,40] Residues T196 and Y197, which are located in the C-terminal hydrophobic groove of major pilins, may involve donor−strand complementation or the donor−strand exchange reaction.[13,14] Therefore, residue V45, T196, and Y197 substitutions of MrkA may also influence the stability of type 3 fimbriae and reduce the number of fimbriae on the cells.

It has been shown that the *K. pneumoniae mrkA* knockout mutant is defective in biofilm formation,[30] although the underlying mechanism is largely unknown. Therefore, it is not clear why the G189A mutant strain displayed weak biofilm-forming activity while producing a normal quantity of type 3 fimbriae. One possible explanation for this phenomenon is that the amino acid substitution results in a conformational alteration of MrkA and hence changes in surface charge distribution and hydrophobicity in the entire fimbria that lead to less efficient attachment of the bacterial cells to the solid surface. This speculation requires further examination.

Although the TEM images revealed that both the G189A and the Y197A fimbriae may be slightly shorter than the wild-type

dx.doi.org/10.1021/la300224w | *Langmuir* 2012, 28, 7428−7435

fimbriae (0.66 and 0.71 μm vs 1.48 μm, Figure 4), further optical tweezers experiments revealed that only the G189A mutant fimbriae exhibited mechanical properties distinct from those of the wild-type fimbriae, especially in their unstable contractibility. This finding is similar to unstable contractions of a single P fimbria after salinity or pH treatments.[18] The unstable contractibility implies that the G189A substitution specially influences the coiling assembly of MrkA into the helixlike fimbrial filaments.

In addition, the DSC thermograms show that the MrkAG189A mutant fimbriae exhibited a relatively smaller enthalpy, although the endothermic peaks of all of the recombinant fimbriae were comparable to that of the wild type at about 68 °C (data not shown). This result further suggests that the helixlike structure of the MrkAG189A fimbriae is obviously more unstable than that of the wild-type fimbriae, but the change in the coiling assembly of the MrkAG189A fimbriae is actually slight. This hypothesis is consistent with a previous report in which the G150A substitution in PapA slightly altered the helical symmetry of the P-type fimbrial rod from 3.28 to 3.29 subunits/turn.[41] This finding indicates that the turn-to-turn interaction of G150A mutant P fimbriae is less rigid than that of wild-type P fimbriae. It has been proposed that instead of being located in the C-terminal hydrophobic groove of PapA to involve the donor−strand exchange reaction between adjacent pilins, G150 would be at the coiling interface of a P-type fimbrial helix between the nth and n + 3rd major pilins.[15] The sequence alignment implies that the G189 residue of MrkA is a possible equivalent of G150 in PapA. Therefore, the G189A substitution of MrkA would also cause abnormal coiling assembly of the pilins into helixlike filaments.

5. CONCLUSIONS

This study individually generated 11 amino acid substitutions on MrkA and examined how they affect the assembly and biomechanical properties of the type 3 fimbriae and the biofilm-forming ability of the recombinant bacteria. Six of these MrkA variants displayed reduced biofilm-forming activity. Among them, C87A substitution showed the most dramatic effect, rendering the bacterial cell incapable of producing type 3 fimbriae, presumably because the mutant MrkA protein is misfolded. Recombinant bacterial strains carrying F34A, V45A, T196A, and Y197A substitutions produced fewer fimbriae than the wild-type strain, probably because of the impairment of the donor−strand complementation/exchange mechanism in the fimbrial assembly. The smaller number of fimbriae on the cell surface may explain why the biofilm activity of these strains is lower than that of the wild type. The weaker biofilm-forming activity of the MrkAG189A variant may partially result from the shorter fimbrial filaments produced by the bacterial strain. The G189A substitution may result in an abnormal MrkA−MrkA interaction and hence reduced stability as revealed by the optical tweezers and the differential scanning calorimetry analyses. In conclusion, this study has demonstrated that the C-terminal β strands of MrkA are required for the assembly and structural stability of fimbriae.

■ ASSOCIATED CONTENT

Ⓢ Supporting Information

Purity of the fimbriae preparation. Details of the TEM images of *E. coli* cells expressing 11 recombinant fimbriae. Formation of monomeric MrkA. Primers used in this study. Uncoiling forces of the recombinant fimbriae. This material is available free of charge via the Internet at http://pubs.acs.org.

■ AUTHOR INFORMATION

Corresponding Author

*(H.-Y.C.) Tel: (886) 3-5742910. Fax: (886) 3-5742910. E-mail: hychang@life.nthu.edu.tw. (L.H.) Tel: (886) 3-5712121 ext. 56161. Fax: (886) 3-5131241. E-mail: long@cc.nctu.edu.tw..

Author Contributions

○These authors contributed equally to this work.

Notes

The authors declare no competing financial interest.

■ ACKNOWLEDGMENTS

We thank Professor Dr. Chung-Shi Yang at the National Health Research Institutes for kindly providing a Hitachi-H7650 EM to generate the preliminary results; the Institute of Molecular Biology, Academia Sinica, for kindly providing an FEI Tecnai G^2 EM; Yu-Ching Chen, Shu-Ping Lee, and Shu-Ping Tasi for EM technical assistance; and Dr. Feng-Chih Chang at the Institute of Applied Chemistry, National Chiao Tung University, for kindly providing a differential scanning calorimetry instrument for calorimetric measurements. This study was supported in part by the National Science Council and Ministry of Education, Taiwan, Republic of China.

■ REFERENCES

(1) Hornick, D. B.; Allen, B. L.; Horn, M. A.; Clegg, S. Adherence to respiratory epithelia by recombinant *Escherichia-coli* expressing *Klebsiella-pneumoniae* type-3 fimbrial gene-products. *Infect. Immun.* **1992**, *60*, 1577−1588.

(2) Snyder, J. A.; Haugen, B. J.; Lockatell, C. V.; Maroncle, N.; Hagan, E. C.; Johnson, D. E.; Welch, R. A.; Mobley, H. L. T. Coordinate expression of fimbriae in uropathogenic *Escherichia coli*. *Infect. Immun.* **2005**, *73*, 7588−7596.

(3) Kline, K. A.; Falker, S.; Dahlberg, S.; Normark, S.; Henriques-Normark, B. Bacterial adhesins in host-microbe interactions. *Cell Host Microbe* **2009**, *5*, 580−592.

(4) Bullitt, E.; Makowski, L. Structural polymorphism of bacterial adhesion pili. *Nature* **1995**, *373*, 164−167.

(5) Jass, J.; Schedin, S.; Fällman, E.; Ohlsson, J.; Nilsson, U. J.; Uhlin, B. E.; Axner, O. Physical properties of *Escherichia coli* P pili measured by optical tweezers. *Biophys. J.* **2004**, *87*, 4271−4283.

(6) Thomas, W. E.; Nilsson, L. M.; Forero, M.; Sokurenko, E. V.; Vogel, V. Shear-dependent 'stick-and-roll' adhesion of type 1 fimbriated *Escherichia coli*. *Mol. Microbiol.* **2004**, *53*, 1545−1557.

(7) Forero, M.; Yakovenko, O.; Sokurenko, E. V.; Thomas, W. E.; Vogel, V. Uncoiling mechanics of *Escherichia coli* type I fimbriae are optimized for catch bonds. *PLoS Biol.* **2006**, *4*, 1509−1516.

(8) Andersson, M.; Uhlin, B. E.; Fällman, E. The biomechanical properties of *E. coli* pili for urinary tract attachment reflect the host environment. *Biophys. J.* **2007**, *93*, 3008−3014.

(9) Chen, F.-J.; Chan, C.-H.; Huang, Y.-J.; Liu, K.-L.; Peng, H.-L.; Chang, H.-Y.; Liou, G.-G.; Yew, T.-R.; Liu, C.-H.; Hsu, K. Y.; Hsu, L. Structural and mechanical properties of *Klebsiella pneumoniae* type 3 fimbriae. *J. Bacteriol.* **2011**, *193*, 1718−1725.

(10) Sauer, F. G.; Remaut, H.; Hultgren, S. J.; Waksman, G. Fiber assembly by the chaperone-usher pathway. *Biochim. Biophys. Acta* **2004**, *1694*, 259−267.

(11) Zavialov, A.; Zav'yalova, G.; Korpela, T.; Zav'yalov, V. FGL chaperone-assembled fimbrial polyadhesins: anti-immune armament of gram-negative bacterial pathogens. *FEMS Microbiol. Rev.* **2007**, *31*, 478−514.

(12) Girardeau, J. P.; Bertin, Y.; Callebaut, I. Conserved structural features in class I major fimbrial subunits (Pilin) in gram-negative bacteria. Molecular basis of classification in seven subfamilies and identification of intrasubfamily sequence signature motifs which might be implicated in quaternary structure. *J. Mol. Evol.* **2000**, *50*, 424−442.
(13) Sauer, F. G.; Futterer, K.; Pinkner, J. S.; Dodson, K. W.; Hultgren, S. J.; Waksman, G. Structural basis of chaperone function and pilus biogenesis. *Science* **1999**, *285*, 1058−1061.
(14) Choudhury, D.; Thompson, A.; Stojanoff, V.; Langermann, S.; Pinkner, J.; Hultgren, S. J.; Knight, S. D. X-ray structure of the FimC-FimH chaperone-adhesin complex from uropathogenic *Escherichia coli*. *Science* **1999**, *285*, 1061−1066.
(15) Mu, X. Q.; Bullitt, E. Structure and assembly of P-pili: a protruding hinge region used for assembly of a bacterial adhesion filament. *Proc. Natl. Acad. Sci. U.S.A.* **2006**, *103*, 9861−9866.
(16) Mu, X. Q.; Jiang, Z. G.; Bullitt, E. Localization of a critical interface for helical rod formation of bacterial adhesion P-pili. *J. Mol. Biol.* **2005**, *346*, 13−20.
(17) Madison, B.; Ofek, I.; Clegg, S.; Abraham, S. N. Type 1 fimbrial shafts of *Escherichia coli* and *Klebsiella pneumoniae* influence sugar-binding specificities of their FimH adhesins. *Infect. Immun.* **1994**, *62*, 843−848.
(18) Andersson, M.; Axner, O.; Almqvist, F.; Uhlin, B. E.; Fällman, E. Physical properties of biopolymers assessed by optical tweezers: analysis of folding and refolding of bacterial pili. *ChemPhysChem* **2008**, *9*, 221−235.
(19) Fällman, E.; Schedin, S.; Jass, J.; Uhlin, B. E.; Axner, O. The unfolding of the P pili quaternary structure by stretching is reversible, not plastic. *EMBO Rep.* **2005**, *6*, 52−56.
(20) Van Molle, I.; Moonens, K.; Garcia-Pino, A.; Buts, L.; De Kerpel, M.; Wyns, L.; Bouckaert, J.; De Greve, H. Structural and thermodynamic characterization of pre- and postpolymerization states in the F4 fimbrial subunit FaeG. *J. Mol. Biol.* **2009**, *394*, 957−967.
(21) Piatek, R.; Bruzdziak, P.; Wojciechowski, M.; Zalewska-Piatek, B.; Kur, J. The noncanonical disulfide bond as the important stabilizing element of the immunoglobulin fold of the Dr fimbrial DraE subunit. *Biochemistry* **2010**, *49*, 1460−1468.
(22) Podschun, R.; Ullmann, U. *Klebsiella* spp. as nosocomial pathogens: epidemiology, taxonomy, typing methods, and pathogenicity factors. *Clin. Microbiol. Rev.* **1998**, *11*, 589−603.
(23) Wu, C.-C.; Huang, Y.-J.; Fung, C.-P.; Peng, H.-L. Regulation of the *Klebsiella pneumoniae* Kpc fimbriae by the site-specific recombinase KpcI. *Microbiology* **2010**, *156*, 1983−1992.
(24) Jagnow, J.; Clegg, S. *Klebsiella pneumoniae* MrkD-mediated biofilm formation on extracellular matrix- and collagencoated surfaces. *Microbiology* **2003**, *149*, 2397−2405.
(25) Tarkkanen, A. M.; Virkola, R.; Clegg, S.; Korhonen, T. K. Binding of the type 3 fimbriae of *Klebsiella pneumoniae* to human endothelial and urinary bladder cells. *Infect. Immun.* **1997**, *65*, 1546−1549.
(26) Chang, B.-J.; Huang, Y.-J.; Chan, C.-H.; Hsu, L.; Peng, H.-L.; Chang, H.-Y.; Yew, T.-R.; Liu, C.-H.; Chi, S. Measurement of the adhesive force between a single *Klebsiella pneumoniae* type 3 fimbria and collagen IV using optical tweezers. *Biochem. Biophys. Res. Commun.* **2006**, *350*, 33−38.
(27) Di Martino, P.; Cafferini, N.; Joly, B.; Darfeuille-Michaud, A. *Klebsiella pneumoniae* type 3 pili facilitate adherence and biofilm formation on abiotic surfaces. *Res. Microbiol.* **2003**, *154*, 9−16.
(28) Ong, C.-L. Y.; Ulett, G. C.; Mabbett, A. N.; Beatson, S. A.; Webb, R. I.; Monaghan, W.; Nimmo, G. R.; Looke, D. F.; McEwan, A. G.; Schembri, M. A. Identification of type 3 fimbriae in uropathogenic *Escherichia coli* reveals a role in biofilm formation. *J. Bacteriol.* **2008**, *190*, 1054−1063.
(29) Schroll, C.; Barken, K. B.; Krogfelt, K. A.; Struve, C. Role of type 1 and type 3 fimbriae in *Klebsiella pneumoniae* biofilm formation. *BMC Microbiol.* **2010**, *10*, 179.
(30) Langstraat, J.; Bohse, M.; Clegg, S. Type 3 fimbrial shaft (MrkA) of *Klebsiella pneumoniae*, but not the fimbrial adhesin (MrkD), facilitates biofilm formation. *Infect. Immun.* **2001**, *69*, 5805−5812.
(31) Huang, Y.-J.; Wu, C.-C.; Chen, M.-C.; Fung, C.-P.; Peng, H.-L. Characterization of the type 3 fimbriae with different MrkD adhesins: possible role of the MrkD containing an RGD motif. *Biochem. Biophys. Res. Commun.* **2006**, *350*, 537−542.
(32) Lin, C.-T.; Huang, Y.-J.; Chu, P.-H.; Hsu, J.-L.; Huang, C.-H.; Peng, H.-L. Identification of an HptB-mediated multi-step phosphorelay in *Pseudomonas aeruginosa* PAO1. *Res. Microbiol.* **2006**, *157*, 169−175.
(33) Liou, G.-G.; Tanny, J. C.; Kruger, R. G.; Walz, T.; Moazed, D. Assembly of the SIR complex and its regulation by O-acetyl-ADP-ribose, a product of NAD-dependent histone deacetylation. *Cell* **2005**, *121*, 515−527.
(34) Berg-Sørensen, K.; Flyvbjerg, H. Power spectrum analysis for optical tweezers. *Rev. Sci. Instrum.* **2004**, *75*, 594−612.
(35) Huang, Y.-J.; Liao, H.-W.; Wu, C.-C.; Peng, H.-L. MrkF is a component of type 3 fimbriae in *Klebsiella pneumoniae*. *Res. Microbiol.* **2009**, *160*, 71−79.
(36) Ye, Y.-S.; Yen, Y.-C.; Cheng, C.-C.; Syu, Y.-J.; Huang, Y.-J.; Chang, F.-C. Polytriazole/clay nanocomposites synthesized using in situ polymerization and click chemistry. *Polymer* **2010**, *51*, 430−436.
(37) Jacob-Dubuisson, F.; Pinkner, J.; Xu, Z.; Striker, R.; Padmanhaban, A.; Hultgren, S. J. PapD chaperone function in pilus biogenesis depends on oxidant and chaperone-like activities of DsbA. *Proc. Natl. Acad. Sci. U.S.A.* **1994**, *91*, 11552−11556.
(38) Remaut, H.; Rose, R. J.; Hannan, T. J.; Hultgren, S. J.; Radford, S. E.; Ashcroft, A. E.; Waksman, G. Donor-strand exchange in chaperone-assisted pilus assembly proceeds through a concerted beta strand displacement mechanism. *Mol. Cell* **2006**, *22*, 831−842.
(39) Verger, D.; Bullitt, E.; Hultgren, S. J.; Waksman, G. Crystal structure of the P pilus rod subunit PapA. *PLoS Pathog.* **2007**, *3*, 674−682.
(40) Soto, G. E.; Dodson, K. W.; Ogg, D.; Liu, C.; Heuser, J.; Knight, S.; Kihlberg, J.; Jones, C. H.; Hultgren, S. J. Periplasmic chaperone recognition motif of subunits mediates quaternary interactions in the pilus. *EMBO J.* **1998**, *17*, 6155−6167.
(41) Bullitt, E.; Jones, C. H.; Striker, R.; Soto, G.; Jacob-Dubuisson, F.; Pinkner, J.; Wick, M. J.; Makowski, L.; Hultgren, S. J. Development of pilus organelle subassemblies in vitro depends on chaperone uncapping of a beta zipper. *Proc. Natl. Acad. Sci. U.S.A.* **1996**, *93*, 12890−12895.